

Compression stress relaxation apparatus for the long-time monitoring of the incremental modulus

Roland H. Horst

Department of Chemical Engineering and Department of Polymer Science and Engineering, University of Massachusetts, Amherst, Massachusetts 01003

Thomas S. Stephens and James E. Coons

Los Alamos National Laboratory, Los Alamos, New Mexico

H. Henning Winter^{a)}

Department of Chemical Engineering and Department of Polymer Science and Engineering, University of Massachusetts, Amherst, Massachusetts 01003

(Received 13 August 2002; accepted 22 July 2003)

A compression apparatus for aging experiments on soft rubbers and foams is presented. The sample is compressed between two parallel surfaces and held there for long-time relaxation studies. The specific purpose of the test is twofold: possible exposure of the sample to aggressive environment under compression during aging and measurement of sample modulus without unloading, i.e., while leaving the sample under constant compression at all times. To determine the restoring force in the compressed sample, the compression strain is modulated with an incremental strain while measuring the force response. The total force gives the compression modulus, and the slope of the force-strain curve allows the determination of the incremental modulus. Stress relaxation data for silicon foam, Dow Corning S-5370 RTV, with 68% void fraction are shown. The modulus of the compressed sample decays over long experimental times of several days. The decay can be described by two relaxation modes, a short mode at 1500 s and a long mode at about 10^5 s. The incremental modulus changes sharply in the first 1000 s (first mode) and then levels off. The apparatus consists of two self-contained components, the removable sample holder (compression jig) and the stationary test station, which performs the modulation of the strain and all measurements (restoring force and incremental modulus). This allows separation of functions. The apparatus design specifically focused on the control of the incremental strain modulation. © 2003 American Institute of Physics. [DOI: 10.1063/1.1611617]

I. INTRODUCTION

Porous polymeric materials (foams) when used in compression generate a restoring force, which not only depends on the compression strain but also on the aging with time and with exposure to elevated temperature and/or to chemical environment. The foam is characterized by void fraction, pore size distribution, pore shape, and rheological properties of the bulk polymer. Open pore foams behave significantly different from closed cell foams. Some foams are in between, being partly open and partly closed. The major areas of application for open cell materials are catalysis, filtration, membranes, tissue scaffolds, and major areas for closed cell materials are thermal insulation and buoyancy. Mechanical insulation (damping), packaging, compressive sealing, and structural support can be achieved with open as well as closed cell foams.

Here the special focus is on the mechanical behavior under long-time compression since, in many applications, porous polymers are in use for many years and knowing their long-term behavior is crucial. Aging is known to affect

thermal¹ and electric insulation, rheological properties, and the ability of the samples to keep their initial dimensions. When stress is removed after a long loading time, a foam sample only slowly reaches its initial dimensions or may even show permanent distortion,² and it might not recover its original compression modulus. This phenomenon is known as “compression set” and is of utmost importance for cellular plastics used in mechanical insulation and upholstery.^{3,4} Similar phenomena have been observed in creep of elastomers.^{5,6} Long-term exposure to stress can partially collapse the foam. This phenomenon makes it necessary to measure the foam properties without unloading. The measurement has to be performed while the foam remains in place.

The long-term mechanical behavior of foams has typically been studied in a test which resembles the application as sealant. In this test, called compression stress relaxation, the sample is sandwiched between two solid parallel surfaces that compress the sample. The resulting stress in the sample produces a restoring force which decreases with time. The test is defined by the imposed strain ϵ , the resulting normal stress, $\sigma(t)$, and the compression modulus E :

$$\epsilon = \frac{H - H_0}{H_0} \quad \text{with } 0 \geq \epsilon > -1,$$

^{a)}Author to whom correspondence should be addressed; electronic mail: winter@ecs.umass.edu

$$\sigma(t) = \frac{F(t)}{A}, \quad (1)$$

$$E = \frac{\sigma}{\epsilon}.$$

The strain ϵ is defined by the relative change of height H of the sample; H_0 is the height without load applied. A typical compression stress relaxation experiment imposes a constant strain while measuring the resulting force $F(t)$. The average normal stress, $\sigma(t)$, is calculated by dividing the restoring force F with the cross-sectional area A of the sample.

For soft foams, the sample's cross section A was found to be practically constant during deformation while the relative density compensated for the decreasing sample thickness

$$\frac{\rho}{\rho_0} \approx \frac{H_0}{H}. \quad (2)$$

The cellular elastic material for which experimental results will be shown below has a low Poisson's ratio, and lateral expansion is small when it is compressed between solid surfaces, even at the maximum experimental strain of 60%.

The compression modulus E is defined as ratio of ϵ and σ , which are both negative. The differential change of the restoring stress with strain is expressed in an incremental modulus

$$E_i = \frac{\partial \sigma}{\partial \epsilon} \quad (3)$$

for the compressed state. E_i is important to know in addition to the conventionally measured compression modulus. For measuring E_i , the large compression strain is modulated by an incremental strain while simultaneously measuring the force. Such superposition of small deformations onto a dominating, large strain have been shown to be useful for exploring the time dependence of viscoelastic properties (relaxation behavior) of molten polymers during flow.^{7,8} Here we will measure the incremental modulus of solids, which remains constant during the short experimental time but will change during the aging process. Knowledge of the incremental modulus is needed for predicting the behavior in long-term applications.

It is important to realize that this compression modulus and the corresponding incremental modulus differ from the true Young's modulus which is measured, for instance, in a compression experiment which allows free lateral expansion of the sample.⁹ The compression experiments of this study do not allow free lateral expansion due to the large solid surfaces, which contain the sample. Tuckner¹⁰ studied this clamping effect by adding sand paper or lubricant between sample and plates. He observed a difference of 25% in the observed modulus. However, this requires lubrication which has not been used in this study.

The restoring force, F , in a compressed sheet of foam is typically measured in a linear rheometer. Long-time experiments, however, require the development of dedicated instruments that hold the foam in compression while measuring the restoring force periodically without unloading the sample. This is achieved by mounting the sample in a com-

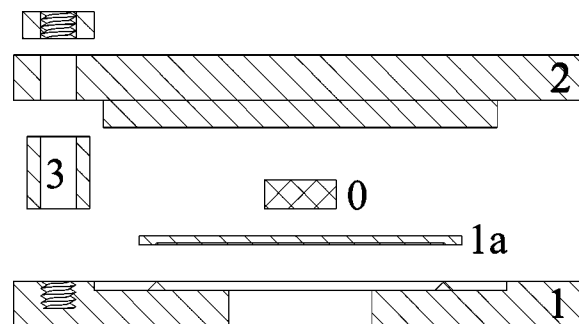


FIG. 1. Cross section of the compression jig. The components are shifted in vertical direction for better visualization: (0) sample, (1) lower flange, (1a) floating plate, (2) upper flange, and (3) spacer. The screw holding the flanges together is not shown.

pression frame (called "jig") with one of the surfaces being mobile (called the "floating plate") as shown in Fig. 1. For the modulus measurement, the floating plate is lifted incrementally while simultaneously measuring the force. As the floating plate loses contact with its support, the applied force balances the restoring force in the foam sample. This instant of separation from the jig's frame can be detected in several ways, e.g., by the break of an electric contact or a change in the slope of the force versus displacement curve, which is measured either in a conventional linear rheometer or in a device especially made for that jig. Tuckner¹⁰ gives an overview of the available compression jigs: The Shawbury Wallace tester and jig is a complete system of measuring device and compression cell with an electrical contact option. Sample height adjustment occurs with a screw in the base of the jig. The Wykeham Farrance system is similar in its functions, but it uses shims to set the compression strain. Tuckner also presents three jigs that can be mounted in a device that measure deflection and load, like the modified Instron tester. The Jamak jig has holes that allow sample exposure to oil. The Jones–Odum jig uses standard 29 mm diam compression set buttons. Furthermore, Tuckner describes a design of reduced size especially for testing while submerged in fluid media. Edmonson¹¹ in his review of methods and fixtures describes the Lucas fixture whose advantages are small size and low cost. Pannikottu *et al.*^{12,13} developed an apparatus especially for tests under cyclic temperature variations. These authors use nonlinear finite element analysis to interpret their data. Two other complete systems are available from Elastocon, Sweden.^{14,15} One is similar to the above technology; the other allows a continuous force measurement, having its transducer permanently connected to the compression cell. In all these different types of compression experiments, the large strain is induced in the sample by sandwiching it in the compression cell. For the force measurement, an incremental strain is added by lifting the floating plate. Except for the Elastocon cell with the force transducer permanently attached all cells should permit aging in aggressive media.

The compression jig of this study is made entirely of stainless steel to enable aging studies in aggressive media. Its simple parts are easy to manufacture and, most importantly, they do not contain any measuring devices. For measurement of displacement and force, the jig gets mounted on a specifi-

cally designed compression stress relaxation apparatus (stand). The restoring force of the foam sample is measured without ever expanding the foam.

The compression stress relaxation apparatus described in this article is specifically designed for soft foams that require extremely high resolution for the measurement of compression strain (displacement measurement) and restoring stress (force measurement). A power train of very high resolution but low maximum torque is used. This high resolution is necessary for measuring the incremental modulus. The apparatus is also designed to study cellular elastic solids at elevated temperatures; the placement of the heated parts at the top of the stand prevents heat convection to the motor or the load cell.

II. MATERIAL

The first samples studied were commercial Dow Corning Silastic 5370 RTV foam (S-5370) supplied as a two-part system. The resin part consists of hydroxyl-terminated polydimethylsiloxane, poly(methylhydrogensiloxane), diphenylmethylsilanol as a blowing agent, and tetrapropoxysilane as a crosslinker. The resin foams and crosslinks upon mixing with the catalyst, stannous bis-2-ethylhexoate. Foaming is caused by hydrogen that is generated from the condensation of hydrogensilane and silanol groups. Crosslinks form by condensation of silanols and tetrapropoxysilane. S-5370 also contains 15 wt % of silica filler, diatomaceous earth.¹⁶ The foam samples have open cells and closed skin layers. The average density is 414 kg/m^3 , which suggests a void fraction of about 68%.

III. DESIGN OF COMPRESSION APPARATUS

The main intention of the design is to provide the highest accuracy possible for long-time measurements of the stress and modulus of a soft polymer. Exposure to aggressive environments over extended periods of time is facilitated by keeping the sample separate from any of the transducers, except during the actual measurement of the modulus. The compression cell can be kept at the aging temperature during the measurement. Different expansion coefficients of the materials do not influence the result; the aging conditions are not interrupted during the measurement.

A. Compression cell (jig)

A cross section of the compression cell can be seen in Fig. 1. The sample rests on a stainless steel disk, the floating plate. The plate is centered by a circular support on the lower flange. A small hole in the center enables a piston to push the floating plate from below. A small circular groove keeps the floating plate aligned with the lower flange. From the top, a stiff plate, the upper flange, comes down onto the sample and is held in place by three screws. Spacers of different thickness enable a range of compressive strains. The upper flange is thicker in the center to enable large compression forces. Our compression cell has an overall diameter of 100 mm and can hold samples up to 50 mm in diameter. All parts of the compression cell consist of stainless steel. The cell is stable

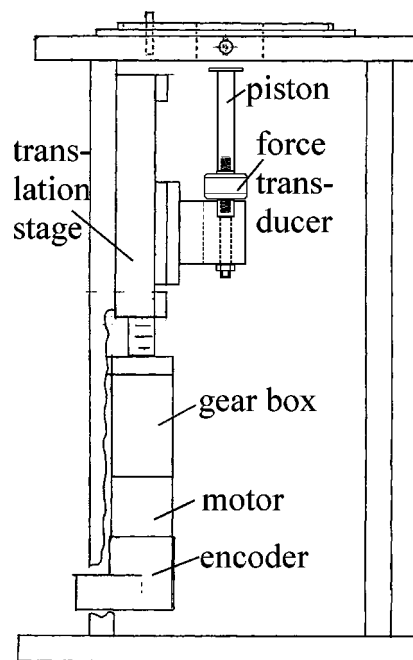


FIG. 2. Cross section of the stand.

and inert in very severe environmental conditions; aging at high temperatures and in most gases causes no problem.

B. Transducer stand

For modulus measurements, the jig gets temporarily mounted onto a stand that contains all transducers. These measure the restoring stress and the incremental strain at a prescribed temperature. The central part of the stand is a translating piston on a microstage with force and displacement measurement, see Fig. 2. A load cell measures the force and an encoder gives the motor position (for the strain). The piston is attached to the sled of a micro stage (MicroStage MS25 of Thomson Industries, W. Springfield, Mass). The main component is a sled sitting on a lead screw that converts the rotational movement of the motor into translation. This stage can withstand forces up to 100 N and is the part that limits the maximum force of the entire apparatus to this value. Motor and lead screw have one common axis. No additional gear is needed, as it would be the case if the motors were positioned horizontally. The motor (model 2842 of MicroMo, Clearwater, Fla.) is equipped with a gearhead 23/1 (gear ratio 246:1) and an optical encoder HEDS-5500A06. The screw has a lead of 0.635 mm; the optical encoder at the motor has a resolution of 500 CPR (lines per revolution), and each count provides four measuring points. This results in a maximum possible resolution of the translational movement of $0.635 \text{ mm}/(500 \cdot 256 \cdot 4) = 1.24 \text{ nm}$, or 806 steps per μm .

An alignment pin in the copper platform provides a good reproducibility of the compression cell's positioning (see Fig. 2). The actual accuracy of the position control was determined by measuring the gap of the compression cell ten times at a typical velocity of the piston of $10 \mu\text{m/s}$. When the jig was not removed between the experiments the standard deviation is $1.7 \mu\text{m}$. If the cell is removed from the stand and

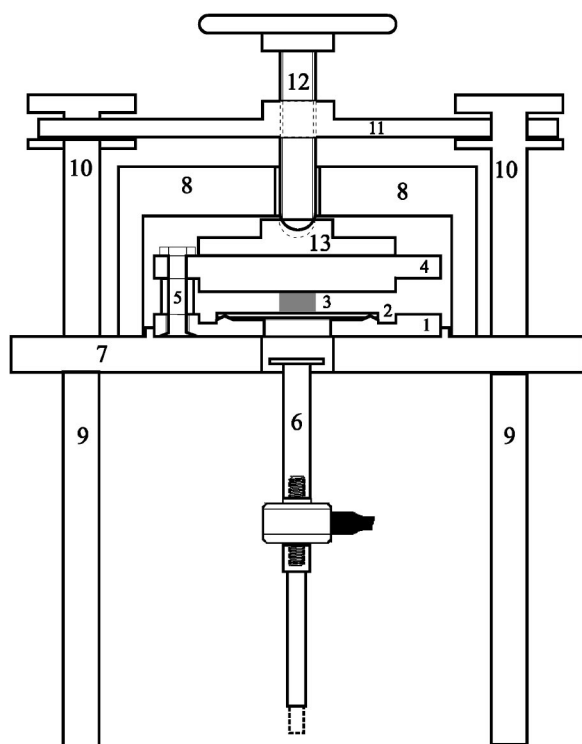


FIG. 3. Cross section of the top of the stand and compression cell: (1) lower flange, (2) floating plate, (3) sample, (4) upper flange, (5) spacer, (6) piston with load cell, (7) copper platform, (8) copper cap, (9) pillar, (10) bracket strut, (11) bracket, (12) pressing screw, and (13) screw jack disk.

set back every time, the standard deviation increases to $7.0 \mu\text{m}$.

During the measurement the piston pushes against the floating plate from below. A simple screw jack press holds the jig down so that it cannot be lifted in its entirety. The top of the piston is electrically insulated from the rest of the piston. This allows a measurement of the electrical contact between piston and stand. This additional information helps in the determination of the experimental curve as will be discussed below. All parts of the stand and the screw jack press are made of aluminum, except for the threaded shaft of the pressing screw.

C. Force measurement

Figure 3 shows the assembly of the stand with compression cell, copper cap, and screw jack press. The load cell with a maximum allowed force of 125 N (Entran Devices, Fairfield, N.J.) is integrated into the piston. The load cell is calibrated with weights of known mass. The measured force has to be corrected for the weight of the sample and of the floating plate.

D. Compliance correction of stand

The setup is not perfectly stiff. To measure its finite compliance, the compression cell was loaded with a solid steel sample and the force was measured as a function of the apparent displacement at the typical velocity of $10 \mu\text{m/s}$. Ideally, one would expect an instantaneous rise of the normal force when the distance between the plates becomes identical to the thickness of the metal spacer. In reality, there is a finite

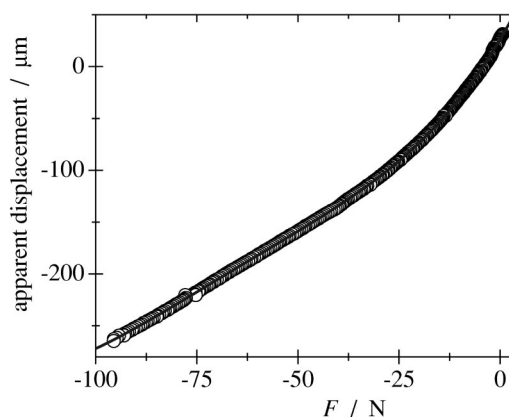


FIG. 4. Apparent displacement change due to the compliance of the apparatus as a function of applied force. The velocity is $10 \mu\text{m/s}$.

slope of force versus displacement. This is due to the fact that the displacement is determined by measuring the revolution of the motor axis rather than a direct measurement of the displacement of the lower plate. When the gap closes, the piston is arrested at a fixed position, assuming the steel spacer is infinitely rigid. As the motor rotates further, the encoder reports increasing “displacements,” even if the piston cannot move; the confined motion of the motor results in a force which compresses the gear train and somewhat stretches the frame. The apparent displacement as a function of force resulting from this calibration experiment with the steel spacer is shown in Fig. 4 and was fitted by a polynomial of fifth order. This apparent displacement, measured at the same velocity that is usually applied for the experiments, is subtracted from the displacement measured by the encoder to give the actual displacement of the lower plate. Upon measuring the steel sample again, the force versus the corrected displacement curve yields a vertical line. All displacement values shown in this paper are corrected for the compliance of the apparatus.

The setup is made very stiff in order to keep the compliance correction small. This is achieved by motor and lead screw of the microstage having a common axis (no gear necessary), and the distance between motor axis and piston being as small as possible to minimize torque on the gear train. For the determination of the incremental modulus, as shown in Fig. 6, the force changes by 0.7 N when the displacement changes by $90 \mu\text{m}$. The compliance correction for these conditions is $3.7 \mu\text{m}$. The stiffness of the apparatus has to be reasonably large compared to the stiffness of the sample, i.e., the present setup is designed for soft materials. If a rubber under investigation would show a very high modulus, the sample cross section has to be kept small to avoid compliance problems. For an incremental modulus of 1.5 MPa and a sample diameter of 12 mm the ratio of the slopes is about 4 and is sufficient for the reproducibility of the experiment.

E. Temperature control

The top of the stand with the compression cell is shown in Fig. 3. The upper part (7: copper platform) is made of a copper plate of $1/2 \text{ in.}$ thickness having a hole in the center that matches up with the hole in the lower flange of the

compression cell. There are two cartridge heaters within the plate, 170 W each. A Watlow 998 Controller regulates the temperature, which is measured by a thermocouple in the centerline of the copper plate. The copper base plate is thermally insulated from the lower parts of the stand by a small piece of glass fiber-reinforced polyester. For maximum stability it is necessary to screw the copper plate onto the pillars of the stand and allow a small heat flow into the pillars and the lower parts of the stand.

The compression cell is covered by a copper cap, which sits on the heated copper plate. The cap also contains two heaters. The high heat conductivity of copper causes a constant temperature around the compression cell. During the measurement, the compression cell is completely surrounded by copper and so the temperature can be kept at the same level as used for the aging. Measuring at different points on the compression cell, a maximum deviation of 2 K from the set point could be determined. The temperature is lowest next to the two central openings in the copper platform and lid.

F. Experimental procedure

The experiment itself is performed by raising the piston with constant speed. It pushes on the sample from below through a hole in the lower flange. The resulting force on the piston is measured with a load cell. The control software runs on a PC and is written in LABVIEW®.

G. Thickness of stress-free sample, H_0

The sample thickness is not easily determined since no sample is completely flat and with parallel surfaces. For our experiments, we take a value of H_0 , which actually comes from an experiment with the compression apparatus, however, by using large spacers in the jig; the spacer length exceeds H_0 . The jig with sample is mounted on the stand and the piston rises at constant speed. The resulting force curve shows a discontinuity when plate and sample are lifted from the support, then it is constant for some time, and increases rapidly when the sample touches the upper flange. The distance between these two points of sudden change in force is the difference between sample height, H_0 , and gap width, d . The zero gap setting for a given spacer thickness has to be determined by performing the same experiment without a sample.

IV. EXPERIMENTAL RESULTS AND DISCUSSION

A. Modulus of stress-free sample

To test the apparatus, a foam sample was compressed in the new compression apparatus and, for comparison, in a linear rheometer (Rheometrics RDSLAs with UMass control, LABVIEW based). Figure 5 compares both experiments. For measurements with the jig, sufficiently tall spacers were used so that the sample was not compressed initially in the fixture. The sample is stress free until the floating plate gets lifted sufficiently and the spacing between the plates, d , is reduced to the sample thickness, H_0 . Then, the (negative) stress starts to rise when further increasing the compression strain (H_0

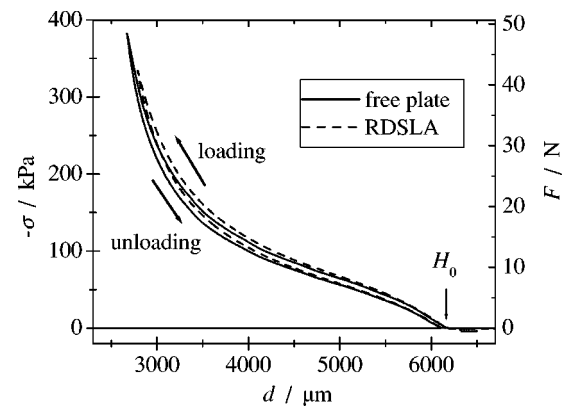


FIG. 5. Dependence of the elongational stress, σ , and the compression force, F , on the separation of plates, i.e., gap thickness, d . Comparison of an experiment with a free floating plate to results obtained in the RDSLAs. The compression speed is $3 \mu\text{m/s}$. The stress for compression is negative. H_0 is the height of the stress-free sample.

– H)/ H_0 . The experiment starts at the right-hand side of the graph where the gap width is larger than the thickness of the sample. The compression curves of the two instruments compare well.

Two instances can be noted specifically for the experiment with the jig, one when the floating plate (with sample) gets lifted from its support and two when it is lifted far enough so that the sample touches the top flange and begins to be compressed. A small discontinuity appears at $6330 \mu\text{m}$ when the piston touches the floating plate and starts to lift it from the support. The force data are shifted so that zero force is assigned to this instant. The displacement shows the actual gap height. At a gap of $6170 \mu\text{m}$ and below, the force starts to increase since the foam sample touches the upper flange and is starting to get compressed. This point of onset marks the height of the sample H_0 . Further piston movement results in the typical compression curve for a cellular elastic polymer. The force rises gradually with increasing strain (decreasing d). The rise is linear at first and then levels off into a plateau region. At further compression, in the approach of the densified bulk state, the force grows steeply and diverges. The experiment is stopped before reaching 400 kPa and the gap is widened again. The velocity of the piston is chosen very slow, only $3 \mu\text{m/s}$. Loading and unloading curves show a hysteresis, which, however, is very small at this low compression rate.

The observed behavior can be rationalized using the tetrahedral model^{17,18} or the cubic cell model¹⁹ for open cell foams. These models attribute the linear elasticity at very small compressions to cell strut bending. The mechanical properties of foams depend on the modulus of the solid cell wall material. The model predicts the leveling off at increased loading. This region is associated with the collapse of the cells where the restoring force is nearly independent of the degree of compression. This is due to buckling of the cell walls and struts. In the densification region opposite cell walls touch. The final slope of this curve should approach the Young's modulus of the pure solid matrix. All cells are totally collapsed and the struts and walls are compressed them-

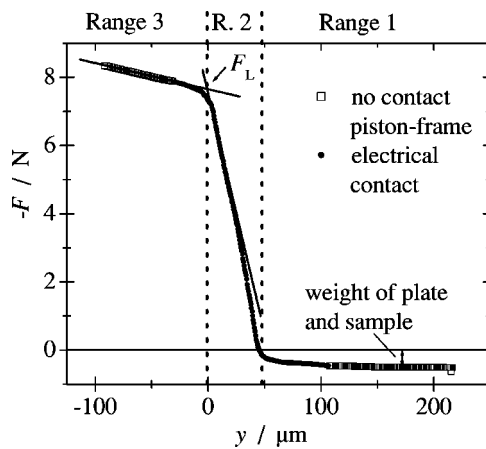


FIG. 6. Dependence of the force F measured by the load cell as a function of displacement y of the piston during loading. y is the vertical direction, moving the piston in negative direction decreases the height of the sample. The sample has a diameter of 12.7 mm and the permanent strain is $\epsilon = -0.17$. The piston speed is $3 \mu\text{m/s}$.

selves. Due to the high density of S-5370, the distinction between the three ranges is not very pronounced.

B. Modulus of compressed sample

For measuring the stress and stiffness in a compressed sample, spacers are chosen to provide the desired compression for the entire duration of the aging process. The compression frame with sample is mounted in the measuring stand for application of an incremental strain by pushing with the piston. A typical measuring curve (Fig. 6, $\epsilon = -0.17$) shows three ranges: (1) At the beginning the piston does not touch the compression cell and the force reading is zero. To correct for the weight of the floating plate and the sample, the initial value is set to the weight force as can be seen in Fig. 6. During the experiment the conductivity between piston and copper plate is measured. In the case where there is no contact, the experimental curve is shown with open symbols, for an electric contact it is plotted with full circles. Since the piston does not touch the floating plate yet, there is no contact. (2) When the piston starts to touch the floating plate there is electrical contact and the load cell registers a force (compression is negative), which increases rapidly with further raising of the piston. (3) In range 3, the plate is lifted from the support and the electrical contact breaks. The sample itself gets compressed by an incremental amount, causing a comparatively slight increase of force with displacement. The electrical contact disrupts only after the slope has completely changed. The reason for the delay might be that there is an electrical contact if plate and support are close enough without touching each other. "Although the electrical contact break allows easy measurement of sealing force, the values determined can be affected by anything that might affect the electrical contact break point, such as sticking or formation of nonconductive surfaces."¹⁰ Indeed, it showed in the experiments of this study that the contact break only works when the points of contact are kept very clean, e.g., cleaning the floating plate and support ring with toluene before starting the assembly. The electrical contact

break is helpful, but not sufficient to determine the separation point.

Ideally, the transition from no-load to sample testing (large force) should occur in a step function, since the displacement is already corrected for apparatus compliance. The transition region in Fig. 6 required a displacement Δy of about $50 \mu\text{m}$. The reason for this nonideal behavior could be several fold: imperfect alignment of piston and compression cell, slight settling of the piston (and the floating plate), or changes in the compliance of the entire setup. Imperfections in flatness and parallelism of the sample should not influence the shape of the transition region, since the sample is held between parallel plates. Effects of backlash were minimized by using a nonbacklash microstage and by always measuring the compliance while moving the piston in the same direction (upward) as during the measurement. Also, during measurements, compression and gravity forces always act in the same direction.

The force, F_L , measured at the intersection of linear extrapolations of ranges 2 and 3 is the compression force at the height of the gap set by the spacers and is taken to be the static force on the compressed foam sample. In Fig. 6, the displacement, y , was shifted so that is zero at this point. The slope in the third range can be directly used to calculate the incremental modulus, E_i :

$$E_i = \frac{\partial \sigma}{\partial \epsilon} = \frac{H_0}{A} \frac{\partial F}{\partial y}, \quad (4)$$

where H_0 and A are the dimensions of the stress-free sample.

C. Modulus decay of compressed foam during aging

Figure 7 shows the stress-strain curves for an aging experiment. The specific set of sample and spacer geometry provides a permanent strain of $\epsilon = -0.465$. At increased aging times, the compression experiment shown in Fig. 6 was performed, see short lines in upper right corner of Fig. 7. The curve for the experiment with a free floating plate is also shown (experiment of Fig. 5).

Figures 8(a)–8(c) show the results of aging experiments at different temperatures at a strain of about 50%. The stress decreases almost linearly in a plot of the stress versus the logarithm of time. Such decay has been reported for other foams.²⁰ The restoring stress in the compressed foam ($\epsilon \approx -0.5$) decays with time over a long time period. The decay is substantial and it continues beyond the experimental times reported here. The initial decay of the modulus is accompanied by a decay of the incremental modulus (solid symbols in Fig. 8). However, the incremental modulus levels off after some characteristic time. The value of compression modulus and incremental modulus do not significantly depend on temperature within the range of the experiments.

The relaxing stress can be represented by three contributions:

$$\frac{\sigma}{\epsilon} = E_\infty + E_f e^{-t/\lambda_f} + E_s e^{-t/\lambda_s} \quad (5)$$

an equilibrium modulus E_∞ reached after a very long time, a fast mode (E_f, λ_f), and a slow mode (E_s, λ_s). The data in

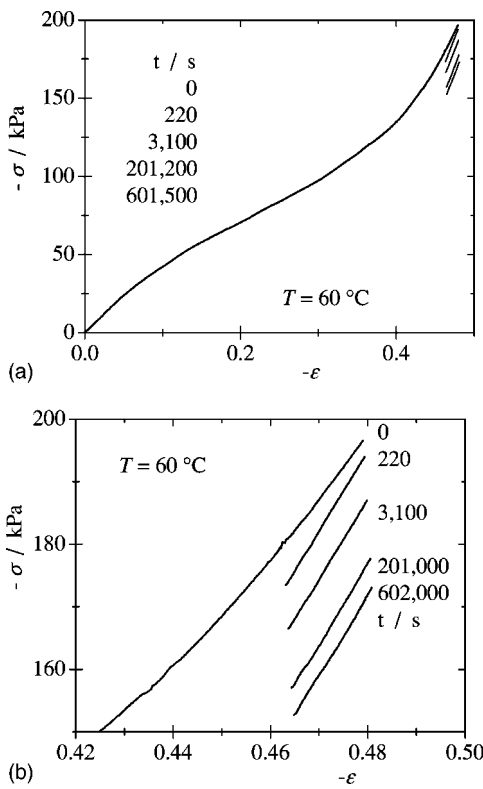


FIG. 7. Dependence of the stress σ on the compressive strain ϵ . All curves measured with increasing $-\epsilon$, i.e., increasing compression. (Top) Complete set of compression experiments. (Bottom) Magnification of upper right section of diagram (incremental modulus measurement). Parameter is the aging time.

Fig. 8 are not extending over long enough a time interval to detect the equilibrium modulus; there might be a distribution of slower relaxations. The modes are listed in Table I. The fast mode turned out to be close to 1500 s for all temperatures and was therefore fixed to this value. The slow mode reflects not exclusively a material property but also the length of the experiment, i.e., the longest lasting experiment gave the longest mode, which limits its physical significance. More experiments are needed at longer times.

Temperature effects are not considered here since the relaxation times for polysiloxane networks typically show only a small temperature dependence,²¹ however, for polysiloxanes crosslinked using tin catalyzed RTV chemistry, chemical stress relaxation is possible.²² The chemical reaction might be the reason for the slow mode.

The incremental modulus decays very rapidly after the initial loading of the sample. Then it maintains its value over long times. It is surprising to see that, even at the very small modulations of the strain [experiment of Figs. 8(a)–8(c)], the incremental modulus is slightly higher for the curves measured with decreasing compression, i.e., increasing sample thickness. At the beginning of the experiment, E_i measured for increasing compression increases, whereas E_i measured for decreasing compression decreases. The reason is that initially the modulus changes very fast. Increasing the absolute value of the strain, the modulus rises but the aging counteracts and so decreases the slope and, therefore, the incremental modulus. Decreasing the strain value, the modulus de-

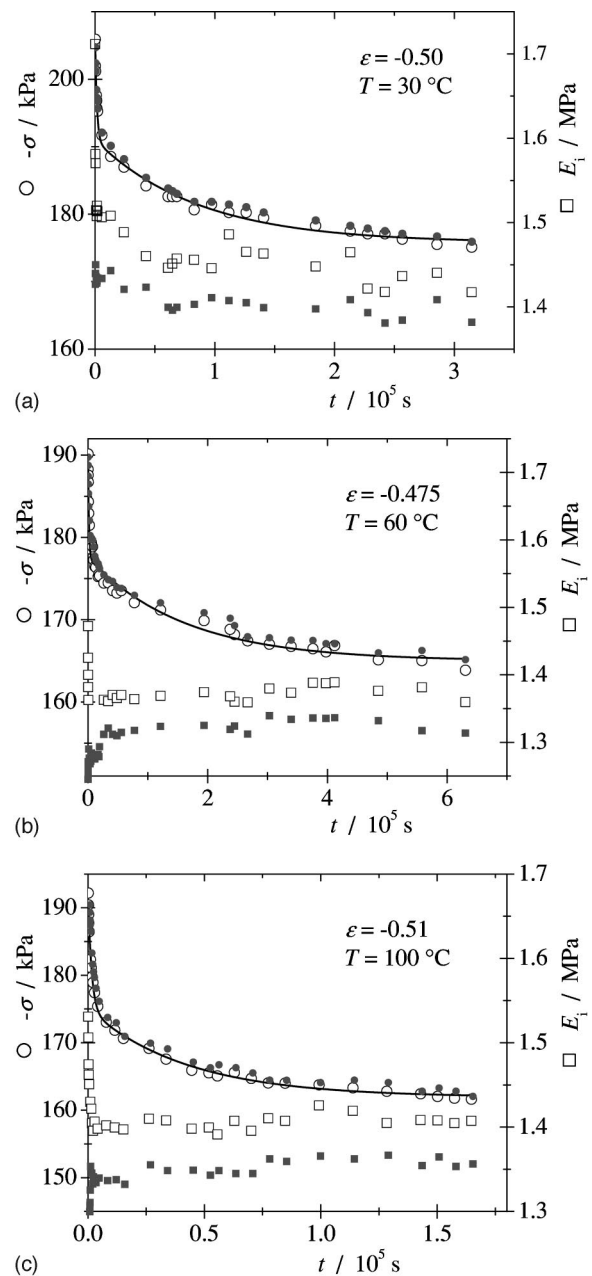


FIG. 8. (a)–(c) Stress relaxation and time dependence of the incremental modulus, E_i , of S-5370 at different temperatures. The solid line is the best fit of Eq. (5) with parameters listed in Table I. (Full symbols) loading, (open symbols) unloading.

creases. Now aging acts in the same direction and the slope is enlarged, E_i becomes larger. Only in the initial range the stress relaxation is fast enough to influence the curves in the way described. As the aging effect on the modulus slows down the incremental moduli for the two measurement directions become similar. The compression stress relaxometer

TABLE I. Relaxation parameters for restoring and incremental stress according to Eq. (3).

$T/^\circ\text{C}$	ϵ	E_∞/MPa	E_f/MPa	$\lambda_f/10^4 \text{ s}$	E_s/MPa	$\lambda_s/10^4 \text{ s}$
30	-0.5	0.351	0.029	0.15	0.031	8.7
60	-0.48	0.344	0.026	0.15	0.026	16.2
100	-0.51	0.318	0.034	0.15	0.026	4.3

is especially built to measure these very slow changes in the material during aging.

The incremental modulus of the present study cannot be directly compared to the incremental modulus of liquids in the study of McKenna and Zapas^{7,8} who apply a large step strain to a polymer solution and then superimpose small strain increments for comparatively short times. In liquids the incremental modulus relaxes very fast and shows a strong time dependence. Their incremental modulus is smaller than the small strain (linear) modulus, but after long experimental times the incremental modulus approaches the conventional modulus as measured in the linear viscoelastic region. This is due to a complete stress relaxation after the large step strain experiment. In the present study where a permanent compression of a solid foam is superimposed with small strain increments, the incremental modulus, E_i , is defined by the slope of $\sigma(\epsilon)$, whereas the conventional modulus E is the slope of the secant to $\sigma(\epsilon)$. In the initial linear range of the compression curve, E_i and E are identical. In the plateau region at large strain, however, E_i is much smaller than E , in the final densification range, E_i is much larger than E .

The solid foam relaxes very slowly, but not completely. Therefore, the linear range is never reached at the high compressions used in the present study. The solid foam relaxes so slowly, that during the short strain increments no time dependence can be observed. The initial strong time dependence of E_i as shown in Fig. 8 is mainly due to the relaxation of the foam during the experiment and is consequently different for E_i determined during increasing and decreasing compression. At later times, the large experimental error of E_i conceals a possible slight time dependence.

Further experiments are needed to clarify the different time dependence of restoring and incremental stress, i.e., the experimental finding that the slow mode is absent for the incremental modulus. Since linear viscoelasticity predicts the same relaxation time distribution for a large or small strain increment, the difference between the relaxation behavior of the stress and incremental modulus measured for S-5370 indicates nonlinear viscoelastic behavior. This is not surprising, since the foam is highly nonlinear in compression.

For the polysiloxane foam studied here, the longest relaxation time appeared to be longer than the experimental time of one week. Since a nonzero equilibrium modulus is expected for cellular plastics with a chemically cross-linked rubber as matrix phase, longer experiments are necessary to determine the equilibrium modulus. This exemplifies the

need for accurate long-time stress relaxation measurements for which this apparatus was designed.

The aging is remarkably different for the compression modulus and the incremental modulus. The compression modulus decays with a very slow mode. This long-time decay is very small or absent for the incremental modulus. This means that the shape of the stress–strain curve changes with aging time. This shows the need for direct measurement of the incremental modulus in long-term aging studies, especially for nonlinear materials. The underlying phenomena for these observations are unknown and require further research.

ACKNOWLEDGMENT

The authors gratefully acknowledge the support of the Los Alamos National Laboratory within the scope of the Enhanced Surveillance Campaign of the Department of Energy.

- ¹ Y. Fan and E. Kokko, *Environ. Int.* **21**, 441 (1995).
- ² P. C. M. Tate and S. Talal, *Polym. Polym. Composites* **7**, 117 (1999).
- ³ J. W. Schneider, *Ind. Chem. Prod. Res. Dev.* **20**, 645 (1981).
- ⁴ J. C. Phillips, *J. Appl. Polym. Sci.* **55**, 527 (1995).
- ⁵ L. C. Brinson and T. S. Gates, NASA Technical Memorandum 109081, N94-29541, 1994.
- ⁶ T. S. Gates and M. Feldman, NASA Technical Memorandum 109114, N94-34396, 1994.
- ⁷ G. B. McKenna and L. J. Zapas, *J. Polym. Sci., Part B: Polym. Phys.* **23**, 1647 (1985).
- ⁸ G. B. McKenna and L. J. Zapas, *Polym. Eng. Sci.* **26**, 725 (1986).
- ⁹ J. D. Ferry, *Viscoelastic Properties of Polymers* (Wiley, New York, 1980).
- ¹⁰ P. Tuckner, Proceedings SAE 2000 World Congress, 2000.
- ¹¹ A. L. Edmondson, Service Life Prediction Forum '97: Two day International Symposium on Advances in Service Life Prediction Techniques for Rubber Components, Thermoplastic Elastomers, Rubber Adhesive Bonds and Rubber Composites, 1997, G1-19.
- ¹² A. Pannikottu, J. A. Seiler, and J. J. Leyden, The 1998 ASME International Mechanical Engineering Congress and Exposition, 1998, DE-Vol. 100.
- ¹³ A. Pannikottu, Y. C. Lu, and M. Centea, Proceedings SAE 2000 World Congress, 2000.
- ¹⁴ G. Spetz, Elastocon AB. How to improve reproducibility 98/2 (1998).
- ¹⁵ G. Spetz, Elastocon AB. Stress Relaxation Tests 98/1 (1998).
- ¹⁶ S. S. Gleiman, T. S. Stephens, R. Mooday, and J. E. Coons, Proceedings AIChE 2000 Annual Meeting, 2000.
- ¹⁷ G. Menges and F. Knipschild, *Polym. Eng. Sci.* **15**, 623 (1975).
- ¹⁸ G. Menges and F. Knipschild, *Stiffness and strength—Rigid plastic foams*, 1982.
- ¹⁹ L. J. Gibson and M. F. Ashby, *Cellular Solids Structure and Properties* (Cambridge University Press, Cambridge, 1997).
- ²⁰ S. L. Hager and T. A. Craig, *J. Cell. Plast.* **28**, 284 (1992).
- ²¹ S. Granick, S. Pederson, S. Nelb, and J. D. Ferry, *J. Polym. Sci., Part B: Polym. Phys.* **19**, 1745 (1981).
- ²² J. Stein and L. C. Prutzman, *J. Appl. Polym. Sci.* **36**, 511 (1988).